Journal of Applied Fluid Mechanics, Vol. 8, No. 3, pp. 483- 489, 2015.
Available online at www.jafmonline.net, ISSN 1735-3572, EISSN 1735-3645.
DOI: 10.18869/acadpub.jafm.67.222.21362

Effect of Periodic Bottom Plate Heating on Large Scale Flow in Turbulent Rayleigh-Bénard Convection

M. Kuqali[1], S. Babuin[2†] and J. J. Niemela[3]

[1] *Polytechnic University of Tirana, Sheshi Nene Tereza 4, Tirana, Albania*
[2] *Institute of Physics ASCR, v.v.i., Na Slovance 2, 182 21 Prague, Czech Republic*
[3] *Abdus Salam International Center for Theoretical Physics, Strada Costiera 11, 34014, Trieste, Italy*

†*Corresponding Author Email: babuin@fzu.cz*

(Received August 02, 2013; accepted August 20, 2014)

ABSTRACT

We report analysis of temperature fluctuations measured inside a Rayleigh-Bénard convection cell of aspect ratio unity with steady and time-varying heating of the bottom boundary. The working fluid is cryogenic helium gas at Rayleigh number $Ra = 10^{13}$, for which a large scale coherent flow (mean wind) exists. We observe the wind to occasionally vanish under both steady and time-varying heating conditions. However, with applied periodic modulation of the lower boundary temperature at the frequency of the wind, we can observe destruction of the periodic temperature variation at the cell mid-plane, due to relative changes in phase between the mean wind and the propagating temperature wave. The wind speed is not observed to change with modulation, demonstrating that it is set by mean properties of the system. Finally we propose that the frequency of the mean wind – and hence the large scale Reynolds number – could be better resolved by finding resonance with applied forcing.

Keywords: Modulated heat; Turbulence; Temperature fluctuations.

1. INTRODUCTION

Rayleigh-Bénard convection is a model for convective flow where the fluid is enclosed within two infinitely wide and infinitely conducting parallel boundaries, the lower one being maintained at a higher temperature than the upper one. We are interested in the highly turbulent regime of such convective flow (Ahlers, Grossmann, and Lohse 2009).

The simplest division of the fluid layer is into three regions: two diffusive boundary layers and a central well-mixed core region (Malkus 1954; Howard 1966). The boundary layers have a time-dependence associated with them due to the periodic emission of plumes, and the plumes themselves lead to a large scale circulation, or mean wind, that encompasses the entire cell and synchronizes the emissions from the two boundary layers (Kadanoff 2001; Niemela, Skrbek, Sreenivasan, and Donnelly 2001; Qiu and Tong 2001). It is of some interest, then, to apply time-periodic forcing to the heating of the lower boundary to examine if the properties of the mean wind could be affected.

The effect of periodic heating on the critical Rayleigh number and the onset convection pattern has been studied by linear stability analysis (Bhadauria and Bhatia 2002) and weakly non-linear stability analysis (Roppo, Davis and Rosenblat 1984; Bhadauria, Bhatia and Debnath 2009).

In this article instead we report an experiment performed in a regime of fully developed turbulence, at Rayleigh number $Ra = 10^{13}$, using cryogenic helium gas in a cell with aspect ratio unity. The Rayleigh number is a non-dimensionalization of the temperature difference ΔT between the boundaries, it quantifies the intensity of convective turbulence, and is defined as $Ra = g\alpha\Delta T h^3/(\kappa\nu)$, where g is the gravitational acceleration, h the vertical separation between the boundaries, and α, κ and ν the thermal expansion, thermal diffusivity and kinematic viscosity of the fluid.

Temperature fluctuations in the bulk have been observed with an emphasis on comparing steady versus time-varying bottom plate heating, with respect to the behavior of the mean wind. An earlier work (Niemela and Sreenivasan 2008) used the modulated boundary temperatures to define the boundaries of a turbulent core region.

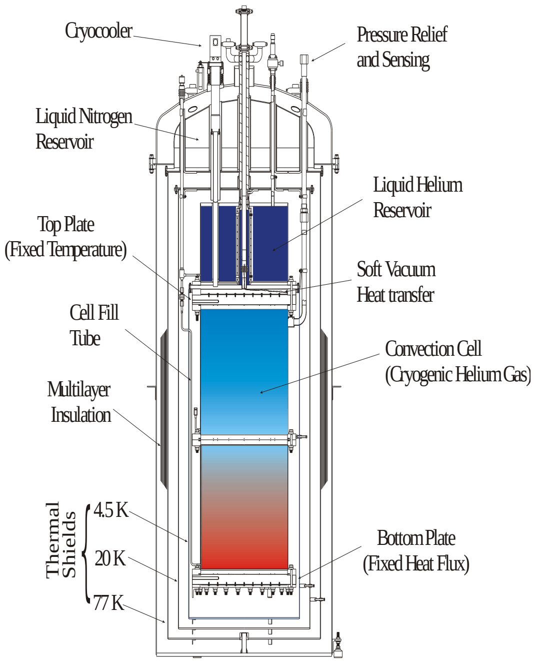

Fig. 1. Schematic diagram of the convection apparatus (Niemela, Skrbek, Sreenivasan, and Donnelly 2000). In the present experiment the cell was half as high as depicted here (see Fig. 2).

2. EXPERIMENTAL APPARATUS AND MEASUREMENT METHOD

The experimental apparatus was the same used by Niemela and co-authors (Niemela, Skrbek, Sreenivasan, and Donnelly 2000) depicted in Figure 1, except that the height of the cylindrical Rayleigh-Bénard convection cell was reduced from 100 cm to 50 cm (aspect ratio unity). It consists of a closed cylindrical container with thick bottom and top plates made of highly conducting annealed copper having a high thermal conductivity of 1 $kWm^{-1}K^{-1}$ near 5 K, which is roughly 5 orders of magnitude larger than that of the helium gas, hence approximating well the condition of an isothermal surface required by the Rayleigh- Bénard paradigm (low Biot number). Thin sidewalls made of type-304 stainless steel enclosed the fluid. The space just above the top plate of the cell was filled with helium gas and served as an adjustable and distributed thermal link between the experiment and the liquid helium reservoir. The apparatus was insulated by three thermal shields at various graded temperatures, 77 K, 20 K and 4.5 K (from the outer to the inner shield respectively) and a common vacuum space to minimize parasitic heat leaks. A further modification consisted in adding an insulating layer of Mylar, 0.127 mm thick, covering the entire inner surface of the stainless steel sidewall of the cell (Niemela and Sreenivasan 2003). The flange region of the joints just above the lower plate and below the upper plate was covered with an additional 2.5 cm wide strip of Mylar of the same thickness. These modifications were intended to further reduce heat conduction along the side walls.

Temperature fluctuations were measured by a matched pair of sensors (see Figure 2) placed a distance w = 4 cm radially inward from the sidewall on the horizontal mid-plane, aligned vertically and separated by a distance d = 2.54 cm. These sensors were bare cubic crystals of Neutron Transmutation Doped germanium, 250 μm on side. Temperature fluctuations were measured simultaneously by separate resistance bridge circuits operated off-balance at frequencies of a few kHz and with an acquisition rate of 100 Hz. The number of data points in a single continuous run was 2^{19}.

We measured temperature fluctuations in the bulk corresponding to two modes of bottom plate heating: DC, and AC of the form $Q = Q_0 + Q_m \sin(2\pi f_m t)$, where Q_0 is a constant heat floor, and Q_m and f_m are the amplitude and frequency of modulation. In both cases, data were measured after statistical steady-state of the temperature of upper and lower plates had been achieved. As a result of heat modulation, the bottom plate temperature also varied periodically with the same frequency of the drive, $T_b = \langle T_b \rangle + \delta T \sin(2\pi f_m t)$, where $\langle\ \rangle$ denotes averaging over time, and δT is the amplitude of the modulation. To characterize our time series we use f_m / f_w, the ratio of modulation frequency to wind frequency, and $\delta T/\Delta T$, where $\Delta T = \langle T_b \rangle - \langle T_t \rangle$ is the difference between time-averaged temperatures of bottom and top plates respectively.

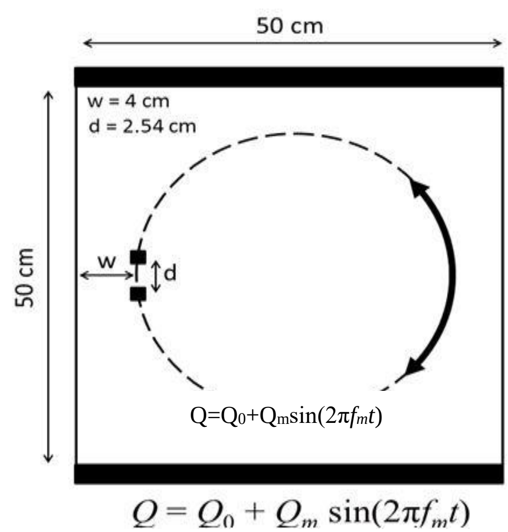

Fig. 2. Schematic diagram of the convection cell with the temperature sensors. The lower boundary is subjected to periodic heating.

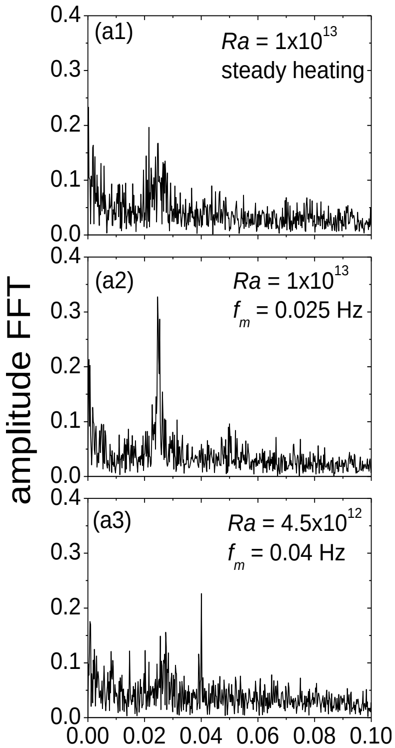

Fig. 3. Amplitude FFT of three emperature fluctuation time series from one sensor of the pair located near the sidewall. The three rows relate to steady heating and modulated heating with forcing frequency (f_m) *at* and *above* the wind frequency. The broad peak around f = 0.025 Hz corresponds to the wind, the narrow peak in (a3) is the forcing frequency.

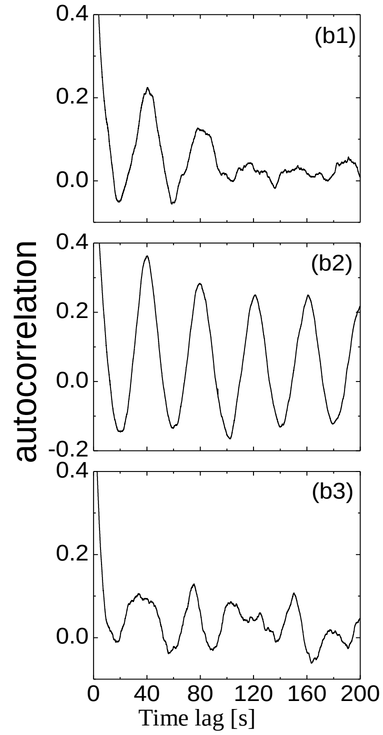

Fig. 4. Autocorrelation of the signal for flow conditions as described in Fig. 3.

3. RESULTS AND DISCUSSION

Figures 3 and 4 display the amplitude Fast Fourier Transform (FFT) and the autocorrelation function (ACF) of temperature fluctuations time series corresponding to three convective flow conditions. Each series was sampled for about 1.5 hrs of real time with one of the sensors in the pair near the side wall. The temperature signal is normalized by subtracting the time average over the whole series and dividing by the standard deviation. The three rows relate espectively to DC heating at $Ra = 1 \times 10^{13}$; AC heating with f_m = 0.025 Hz, $f_m/f_w = 1$, $\delta T/\Delta T = 0.98$ at $Ra = 1 \text{ x } 10^{13}$; and AC heating with f_m = 0.04 Hz, f_m/f_w = 1.6, $\delta T/\Delta T = 0.82$ at $Ra = 4.5 \times 10^{12}$.

First we note that, despite the strong fluctuations present at such high *Ra* when the bulk is highly turbulent and mixed, a coherent circulation is observed to exist on average in all three flow conditions. This is shown by the broad FFT peak centered around f_w = 0.025 Hz.

As shown in particular by the ACF, the coherence of such circulation is enhanced or reduced by modulating the bottom plate heating respectively *at* or *above* the wind frequency. In (a3) the narrow peak at f_w = 0.04 Hz is the forcing frequency.

The broadness of the FFT peak around f_w = 0.025 Hz suggests the existence of several frequency components. To examine this we split each time series into 32 segments of 2^{14} points each, so that each segment has the duration of about four wind turn over times (~ 4 × 40 s) as a minimum window size. On each segment we calculated the ACF and displayed the wind period per segment in Figure 5, for the three flow conditions. Despite the choice of window size is arbitrary, this Figure indicates that there are time intervals during which the correlation is too poor to yield a peak in the ACF, i.e. despite on average the wind is present, there are times when it is discontinued, both in conditions of DC and AC heating. Moreover, the distribution of wind period per segment reflects the components of the broad FFT peak.

The loss of wind coherence in DC conditions is in itself remarkable and was already studied in connection to wind direction reversals (Niemela, Skrbek, Sreenivasan, and Donnelly 2001; Bershadskii, Niemela, and Sreenivasan 2002), however here we are particularly interested in the loss of coherence even when the periodic heat forcing at the bottom plate is maintained at all times. This is clearly demonstrated in

Fig. 6 where we compare the ACF from two segments from the same AC modulation run: the correlation is good in segment 8, but destroyed in segment 11.

A further piece of information comes from returning to the full time series and considering its ACF, shown at the top of Figure 7. The strong correlation with 40 s periodicity (see inset) is present, but it vanishes at almost regular intervals, producing a pattern reminiscent of beating phenomena. To account for these facts we hypothesize destructive/constructive interference occurring between the propagating temperature wave and the mean wind. Indeed, the phase of the propagating wave is dependent on thermal properties of the fluid which effectively change at the interface of the boundary layer and the bulk, an interface which itself is time-dependent due to the periodic depletion of the boundary layer by plume emission.

3.1 Simulations

To test the above hypothesis, we have computed the ACF of the sum of two waves constructed to mimic the modulation of the bottom plate heating and the mean wind periodicity. The superposition function is

$$\Psi = \Psi_1 \sin(2\pi f_1 t + \varphi_1) + \Psi_2 \sin(2\pi f_2 t + \varphi_2) \quad (1)$$

For the case of AC heating at the wind frequency, we have fixed $f_1 = f_m = 0.025$ Hz to represent the frequency of modulation, which in the experiment is set. We then allowed f_2 to vary slightly around f_1, to represent the frequency of the mean wind. We have therefore computed the ACF of Ψ for several choices of the other parameters. The case with $f_2 = 0.0256$ Hz, $\Psi_1 = \Psi_2 = 1$, and $\phi_1 = \phi_2 = \pi$ is shown in Fig. 7.

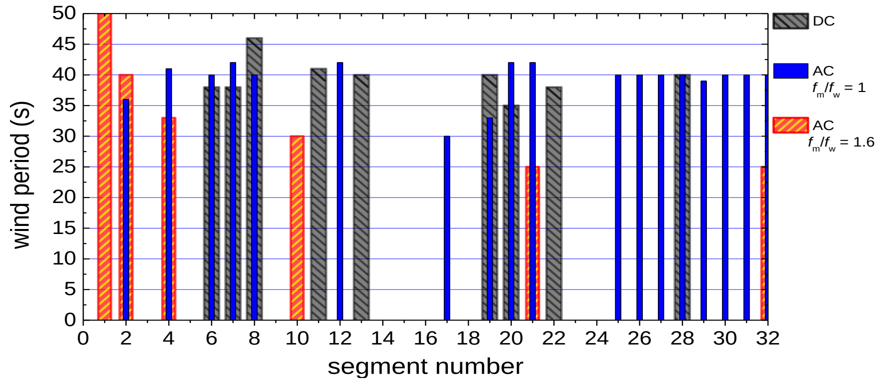

Fig. 5. (Color online) The period of the mean wind for each segment of a split time series, for the three flow conditions.

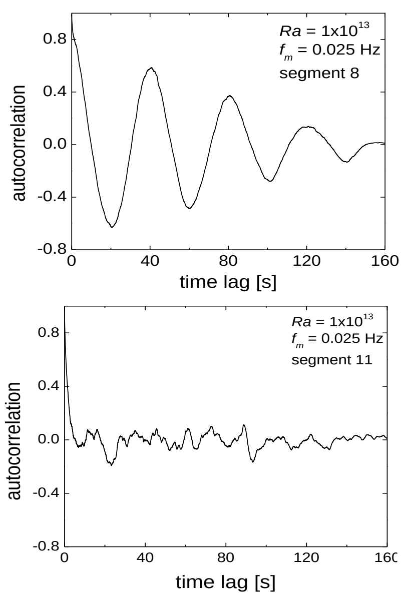

Fig. 6. ACF of two segments taken from the time series sampled with AC forcing with $f_m/f_w = 1$.

We have repeated this approach for the case of AC heating above the wind frequency, and the results are in Figure 8, fixing $f_1 = f_m = 0.04$ Hz and using the following set of optimized parameters: $f_2 = 0.027$ Hz, $\Psi_1 = 1.1$, $\Psi_2 = 1$ and $\phi_1 = \phi_2 = \pi$.

The good agreement between experiment and simulation suggests that our hypothesis may be valid. In the case of $f_m/f_w \approx 1$ the bottom plate drives convection at a frequency which is similar, but not identical, to the frequency of the large scale circulation; this causes beating resulting in alternating suppression and enhancement of the mean wind. Similarly, in the case of $f_m/f_w = 1.6$ the poorer coherence caused by driving the heat off wind resonance is reproduced by the model.

From these observations we can draw the following conclusions for the behavior of the mean wind at high *Ra*. First, it is not steady and occasionally is completely extinguished. This was evident also from the measurements in the absence of modulation of the bottom plate. Second, there is an occasional nearly destructive interference between the mean wind and the modulation signal at the level of the midplane (and by the same argument also enhancement). This is evidenced by the complete lack of correlation (or enhancement) occasionally measured, given that the applied modulation is fixed and steady. This is likely due to changes in phase of the modulated signal which propagates across a boundary layer of varying thickness due to plume emission, resulting into the temperature wave reaching the bulk earlier or later at successive cycles. The jump in phase is experienced at the interface with the bulk which has an effectively larger diffusivity of heat.

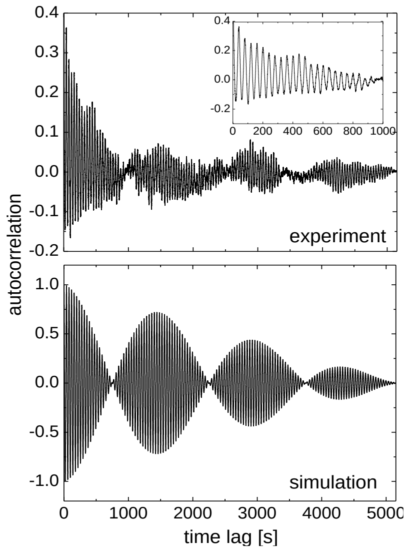

Fig. 7. (top) Experiment: ACF of full temperature fluctuations time series from modulated heating with $f_m/f_w = 1$, at $Ra = 1 \times 10^{13}$. In the inset, zoom of the first 1000 s; (bottom) Simulation: ACF of superposition of two waves of very similar frequency. Similarity between experiment and simulation suggests that propagating temperature wave and mean wind interfere constructively and destructively.

The reduction and enhancement of heat and mass transport upon applying a sinusoidal heating at one boundary has also been demonstrated numerically for a different but related convective system (El Ayachi *et al.* 2010).

3.1 Wind velocity

Our technique allows also for measurements of mean wind velocity by correlating the temperature fluctuations simultaneously sampled at the two neighboring thermometers in Fig.2 (Niemela, Skrbek, Sreenivasan, and Donnelly 2001). The idea is that if a coherent wind blows past the two sensors, then structures in the temperature fluctuation time series detected by one sensor should reappear with a time shift at the position of the other, which is a known distance away in the vertical direction (the direction of the wind at the midplane). Let $T_1(t_i)$ and $T_2(t_i)$ be the two simultaneously sampled temperature time series, where t_i is the i-th step of discretized time. Then we define the correlation function

$$G(\tau) = \sum_{i=1}^{N} T_1(t_i) T_2(t_{i+n}) \qquad (2)$$

where $\tau = t_{i+n} - t_i$, and the window size N is tunable and generally similar to the wind turnover time (30 - 40 s). We find the optimum τ (which can be also negative) for which G is maximum, and thus the mean wind velocity is defined as $v = d / \tau$, where $d = 2.54$ cm is the separation between sensors. We have calculated v for the three flow conditions discussed so far, using the full time series. The normalized probability density function (PDF) of v is shown in Figure 9. First of all we note that the wind can have velocity of opposite sign at the fixed location of the sensors, which reflects the fact that it sometimes reverses direction (Niemela, Skrbek, Sreenivasan, and Donnelly 2001; Bershadskii, Niemela, and Sreenivasan 2002), but this is not our main concern here. Secondly, we note that both steady and modulated heating at the frequency of the wind produce similar, bi-modal distributions (with a slight tendency for negative velocity circulation events). It appears that modulation at a frequency higher than the wind frequency diminishes the amount of time the circulation is in the positive direction, but this could also be an artifact of finite sampling. Finite sampling problems can come about because the reversals do not occur periodically and the time between successive reversals can vary from one circulation time to hundreds (Niemela, Skrbek, Sreenivasan, and Donnelly 2001). This is illustrated in Figure 10, where the wind velocity is plotted as a function of time. One can see clearly that the time scale associated with reversals of the direction of the mean wind can be long and that reversals are not periodic.

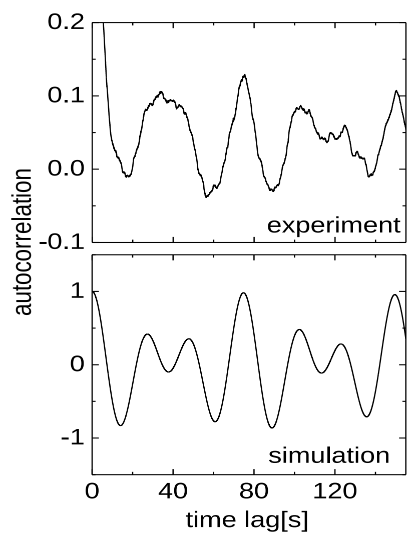

Fig. 8. (top) Experiment: ACF of full temperature fluctuations time series from modulated heating with $f_m/f_w = 1.6$ and $Ra = 4.5 \times 10^{12}$; (bottom) Simulation: ACF of superposition of two waves representing respectively the forcing frequency and the wind frequency.

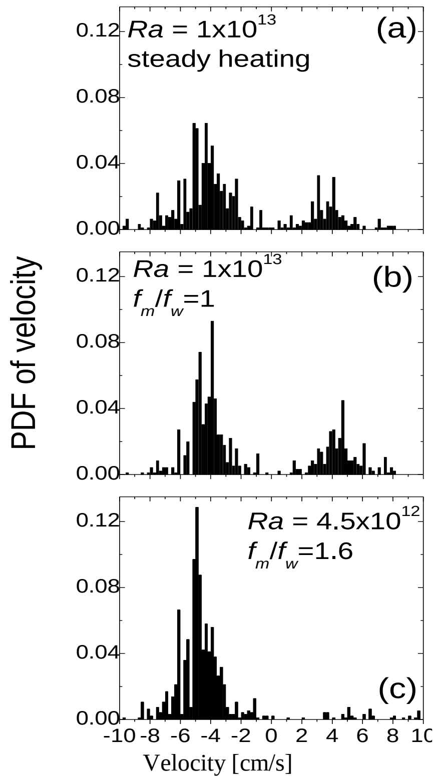

Fig. 9. Normalized probability density function of mean wind velocity for three heating conditions. The velocity is calculated from correlating temperature fluctuation signals from two neighbouring thermometers, as described in the text.

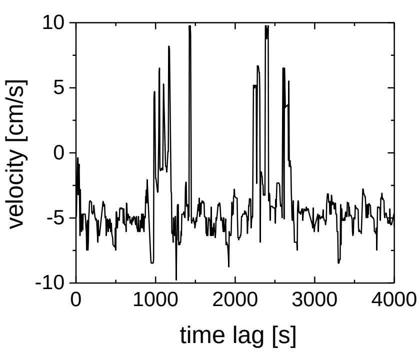

Fig. 10. Wind velocity as a function of time at *Ra* = 4.5×10^{12} and $f_m/f_w = 1.6$.

4. CONCLUSIONS

In this study we have examined the effect of imposing a periodic modulation of the bottom plate heating in a turbulent Rayleigh-Bénard convection system, using cryogenic helium gas at high Rayleigh number $Ra = 10^{13}$. In particular we have focused on the effect of modulating the drive at, or just above, the frequency of the weakly coherent large scale circulation (mean wind) observed to exist in conditions of steady heating.

The wind is observed to reverse its direction of circulation both in steady and time-varying heating conditions. We have shown that reversal statistics over the course of hours can be widely variable, therefore whether and how modulation significantly affects the statistics of the wind reversals cannot currently be established. What is more certain is that the modulation of the convective forcing does not significantly affect the magnitude of the wind velocity. This reinforces the notion that the wind speed (or Reynolds number) is determined by mean properties of the flow and/or fluid.

The actual existence of the mean wind, however, is due to the regular and periodic emission of plumes from two coupled boundary layers at the top and bottom of the cell. When one of those boundaries is subject to a periodic and strong oscillation of temperature, so that local and instantaneous buoyancy is affected, the wind is seen to survive. We find that the measured periodicity in fact does not change with heat modulation, which is due to the fact noted above that the wind speed is determined by the mean state of the system, coupled with the fact that the circulation must traverse the entire circumference of the cell. On the other hand the heat modulation does affect the wind in the sense that their relative phase can change, giving rise to situations where there is destructive or constructive interference between them, resulting respectively into lack of - or enhancement of - large scale coherence.

As a final conclusion we can propose that applied sinusoidal forcing could be used to resolve better the frequency of the mean wind through finding resonance, as the modulation frequency is swept through nearby values.

ACKNOWLEDGEMENTS

One of us (MK) acknowledges a fellowship offered by the Sandwich Training Educational Programme (STEP) with financial support provided by the ICTP and IAEA. MK also expresses sincere gratitude to prof. Pellumb Berberi from the Polytechnic University of Tirana for precious guidance.

REFERENCES

Ahlers, G., S. Grossmann, and D. Lohse (2009). Heat transfer and large scale dynamics in turbulent Rayleigh-Bénard convection. *Rev. Modern Phys. 81*, 503–537.

Bershadskii, A., J. J. Niemela, and K. R. Sreenivasan (2002). Mean wind and its reversal in thermal convection. *Phys. Rev. E 65*, 056306.

Bhadauria, B. S., and P. K. Bhatia (2002). Time periodic heating of Rayleigh-Benard convection. *Physica Scripta*, *66*, 59.

Bhadauria, B. S., P. K. Bhatia, and L. Debnath (2009). Weakly non-linear analysis of Rayleigh-Bénard convection with time periodic heating. *Int. J. of Non-linear Mech. 44*, 58 - 65.

El Ayachi, R., A. Raji, M. Hasnaoui, A. Abdelbaki, and M. Naïmi (2010). Resonance of double-diffusive convection in a porous medium heated with a sinusoidal exciting temperature. *J. of Applied Fluid Mech. 3*, 43-52.

Howard, L. (1966). Convection at high Rayleigh numbers. In H. Görtler (Ed.), *11th Int. Cong. Appl. Mech.*, Berlin. Springer.

Kadanoff, L. (2001). Turbulent heat flow: Structures and scaling. *Physics Today 54*, 34.

Malkus, W. V. R. (1954). Heat transport and spectrum of thermal turbulence. *Proc. R. Soc. Lond. A 225*, 196.

Niemela, J. J., L. Skrbek, K. R. Sreenivasan, and R. J. Donnelly (2000). Turbulent convection at very high Rayleigh numbers. *Nature 404*, 837.

Niemela, J. J., L. Skrbek, K. R. Sreenivasan, and R. J. Donnelly (2001). The wind in confined thermal convection. *J. Fluid Mech. 449*, 169.

Niemela, J. J. and K. R. Sreenivasan (2003). Confined turbulent convection. *J. Fluid Mech. 481*, 355–384.

Niemela, J.J. and K.R. Sreenivasan (2008). Formation of the “superconducting” core in turbulent thermal convection. *Phys. Rev. Lett. 100*, 184502.

Roppo, M. N., S. H. Davis, and S. Rosenblat (1984). Bénard convection with time-periodic heating. *Physics of Fluids 27*, 796.

Qiu, X. L. and P. Tong (2001). Coherent oscillations in turbulent rayleigh-benard convection. *Phys. Rev. Lett. 87*, 094501.